REGULAR ARTICLE

blood advances

E_μ and 3′RR transcriptional enhancers of the IgH locus cooperate to promote c-myc–induced mature B-cell lymphomas

Nour Ghazzaui,* Hussein Issaoui,* Mélissa Ferrad,* Claire Carrion, Jeanne Cook-Moreau, Yves Denizot,† and François Boyer†

Unité Mixte de Recherche Centre National de la Recherche Scientifique 7276, Institut National de la Santé et de la Recherche Médicale U1262, Equipe Labellisée Ligue 2018, Université de Limoges, Limoges, France

Key Points

- Transcriptional cooperation between IgH E_μ and 3′RR enhancers is found during B-cell lymphomagenesis in IgH-c-myc mice.
- Transcriptome analysis reveals wide similarities between human and mouse Burkitt B-cell lymphomas.

Numerous B-cell lymphomas feature translocations linking oncogenes to different locations in the immunoglobulin heavy chain (IgH) locus. During Burkitt lymphoma (BL), IgH breakpoints for c-myc translocation stand either close to J_H segments or within switch regions. Transcription, accessibility, and remodeling of the IgH locus are under the control of the 2 potent *cis*-acting enhancer elements: E_μ and the 3′ regulatory region (3′RR). To ensure their respective contributions to oncogene deregulation in the context of the endogenous IgH locus, we studied transgenic mice harboring a knock-in of c-myc in various positions of the IgH locus (3′ to J_H segments, 5′ to C_μ with E_μ deletion and C_α). The observed spectrum of tumors, kinetics of emergence, and transcriptome analysis provide strong evidence that both E_μ and 3′RR deregulate c-myc and cooperate together to promote B-cell lymphomagenesis. Transgenics mimicking endemic BL (with c-myc placed 3′ to J_H segments) exhibited the highest rate of B-cell lymphoma emergence, the highest Ki67 index of proliferation, and the highest transcriptomic similarities to human BL. The 3′RR enhancer alone deregulated c-myc and initiated the development of BL-like lymphomas, suggesting that its targeting would be of therapeutic interest to reduce c-myc oncogenicity in vivo.

Introduction

c-myc plays a critical role in cell proliferation, apoptosis, differentiation, metabolism, and genomic instability.[1] Burkitt lymphoma (BL) is characterized by chromosomal translocations involving the c-myc gene and 1 of the immunoglobulin (Ig) loci.[2] Once translocated and having lost its normal control, c-myc is constitutively expressed throughout the cell cycle in B cells. In 80% of cases, the translocation involves the IgH locus, itself regulated by a complex interplay of regulatory elements responsible for tissue- and stage-specific regulation of both transcription and rearrangements. The oncogenic deregulation is considered, only with partial scientific validation, to result from juxtaposition to IgH enhancers.[3] Two potent *cis*-acting elements are proposed for c-myc deregulation in BL: the intronic E_μ enhancer and the 3′RR. E_μ is the key transcriptional regulatory element for efficient variable-diversity-junction (VDJ) recombination.[4,5] Associated with c-myc, E_μ has been shown to promote B-cell malignancies with a pro-B phenotype.[3,6] The 3′RR encompasses the 4 transcriptional enhancers, hs3a, hs1,2, hs3b, and hs4; controls μ transcription in mature B cells[7]; and is the master control element of conventional class switch recombination (CSR),[8,9] locus suicide recombination,[10] and somatic hypermutation,[11] but with little role in VDJ recombination except for silencing early transcription in pro-B cells.[12-14] In conjunction with c-myc, the 3′RR promotes B-cell malignancies with a mature B-cell phenotype.[3,15-17]

In B-cell lymphomas, c-myc is inserted in various positions of the IgH locus. IgH locus breakpoints are located in either the VDJ (endemic BL) or the switch (S) regions (sporadic BL and myelomas). When

Submitted 27 August 2019; accepted 12 November 2019; published online 3 January 2020. DOI 10.1182/bloodadvances.2019000845.

*N.G., H.I., and M.F. contributed equally to this study.

†Y.D. and F.B. contributed equally to this study.

RNAseq data reported in this article have been deposited in the Gene Expression Omnibus database (accession number GSE132721).

The full-text version of this article contains a data supplement.

upstream of E_μ, chromosomal breakage may result from abnormal somatic hypermutation. Breakpoints located within S regions are initiated by an erroneous CSR and link c-myc to a downstream portion of the locus lacking E_μ. Thus, the 3′RR is always conserved on the c-myc translocated chromosome. During B-cell maturation, IgH intrachromosomal interactions were found between the 3′RR and the E_μ enhancer, despite their 200-kb distance on the chromosome.[18] To ensure the real contribution of these enhancer elements in c-myc deregulation in the context of the IgH locus, we studied transgenic mice harboring a knock-in (KI) of c-myc in various positions of this locus. The observed spectrum of tumors, kinetics of emergence, and transcriptome analysis provide strong evidence that both E_μ and 3′RR deregulate c-myc and cooperate together to promote B-cell lymphomagenesis.

Materials and methods

Transgenic mice

Mice housing and procedures were conducted in agreement with European Directive 2010/63/EU on animals used for scientific purposes, applied in France as the "Décret n°2012-118 du 1er février 2013 relatif à la protection des animaux utilisés à des fins scientifiques." Accordingly, the present project (APAFiS≠13855) was authorized by the Ministère de l'Education Nationale, de l'Enseignement Supérieur et de la Recherche, and reviewed by the ethics committee of the University of Limoges. Thus, all methods in the current study were carried out in accordance with relevant guidelines and regulations, and all experimental protocols were approved by French institutions. Three transgenic models (c-myc-KIE_μ, c-myc-KIC_μ, and c-myc-KIC_α) were used. c-myc-KIE_μ mice have a c-myc KI upstream of the E_μ enhancer.[19] c-myc-KIC_μ mice have a c-myc KI upstream of the C_μ gene with deletion of the E_μ enhancer.[20] c-myc-KIC_α mice have a c-myc KI within C_α exons.[21]

B-cell purification

For studies evaluating proliferation, apoptosis, and mRNA expression, splenic B cells were purified using CD43-coupled beads from Miltenyi Biotec (Bergisch Gladbach, Germany) according to the manufacturer's recommendations. Bone marrow immature B cells were recovered from CD23-depleted cells (Miltenyi Biotec) with the EasySep mouse B-cell isolation Kit (STEMCELL Technologies) designed to isolate B cells from single-cell suspensions by negative selection.

Proliferation analysis

$CD43^-$ splenic B-cells (1×10^5 cells/well) were cultured (in sextuplicates) in 96-well plates in Dulbecco's modified Eagle medium supplemented with 10% fetal calf serum, glutamine, nonessential amino acids, and antibiotics either alone or in the presence of lipopolysaccharide (LPS) (0.5 μg/mL) plus anti-CD40 (0.1 μg/mL) for 72 hours. The number of viable cells was assessed using the CellTiter 96 One Solution Cell Proliferation assay (Promega Corporation) according to the manufacturer's recommendations.

Apoptosis assay

Freshly isolated $CD43^-$ B-splenocytes (1×10^6 cells/mL) were cultured in growth medium (Dulbecco's modified Eagle medium supplemented with 10% fetal calf serum, glutamine, nonessential amino acids, and antibiotics) with 0.01 μM H_2O_2 in 24-well plates. Immediately after isolation and after 24 hours'growth, cells were incubated (15 minutes, 4°C) with 7-aminoactinomycine D and fluorescein isothiocyanate-labeled Annexin V antibodies (Becton Dickinson), and analyzed by flow cytometry.

mRNA expression

Total RNA was extracted using Trisol (Thermo Fisher Scientific) according to the manufacturer's instructions. RNA was reverse-transcribed into cDNA by the addition of reverse transcriptase (2 μg total RNA, 20 μL final volume). Quantitative polymerase chain reaction (QPCR) was performed in duplicate by using TaqMan assay reagents, and analyzed on an ABI Prism 7000 system (Applied Biosystems, Foster City, CA). Product references for c-myc and GAPDH were Mm00487803-m1 and Mm99999915-g1, respectively (Applied Biosystems).

Clonality assay

Genomic DNA extracted from tumors was amplified by PCR with the OneTaq DNA polymerase from New England Biolabs (Evry, France). The following primers were used: forward primers: V_HJ558 5′-GCGAAGCTTARGCCTGGGRCTTCA GTGAAG-3′; reverse primer: J_{H4} 5′-AGGCTCTGAGATCCCTAGACAG-3′. PCR parameters: 95°C for 2 minutes (1 cycle); 95°C for 30 seconds, 60°C for 30 seconds, 68°C for 2 minutes (40 cycles); 68°C for 10 minutes (1 cycle). PCR products were migrated on a 2% agarose gel.

Next-generation sequencing for repertoire analysis

Repertoire analysis was carried out on RNA from mouse tumor or spleen samples after RACE PCR and library preparation. Total RNA was extracted using Trisol (Thermo Fisher Scientific) according to manufacturer's instructions. RACE was performed on 250 ng RNA incubated at 72°C for 3 minutes and at 42°C for 2 minutes with a specific mouse $C_H1\mu$-rev downstream primer and 1 μL dNTP (10 Mm; MP Biomedicals). Caprace forward primer, dithiothreitol, 5X ProtoScript buffer, and ProtoScript enzyme (BioLabs) were added to the mixture and incubated at 42°C for 90 minutes and then at 70°C for 10 minutes. Libraries were prepared on RACE products, using an upstream mix of 2 Cμ-reverse specific primers (Cμ-rev1, Cμ-rev 2) and a mix of 2 forward primers (UnivShortFw, UnivLongFw; supplemental Table 1). For PCR, DNA was denatured 30 seconds at 98°C and then submitted to 30 cycles consisting of 98°C for 10 seconds, 65°C for 30 seconds, and 72°C for 30 seconds, and followed by 72°C for 5 minutes as a final step. Next, 400- to 600-bp PCR products were purified from gels using PCR clean-up kit (Macherey-Nagel). Purified PCR products were used to perform another PCR round using primers with adapters (supplemental Table 1). Amplification was performed with Phusion High-Fidelity DNA Polymerase (New England Biolabs) according to the following program: DNA was denatured 30 seconds at 98°C and then submitted to 12 cycles consisting of 98°C for 10 seconds, 62°C for 30 seconds, and 72°C for 30 seconds, and 1 cycle at 72°C for 5 minutes. Next, 400- to 600-bp PCR products were purified from gels using PCR clean-up kit (Macherey-Nagel). Purified PCR products (20 ng) were sequenced on an Illumina Miseq sequencer as previously reported.[22]

RNAseq analysis

LPS-stimulated and unstimulated B-cell splenocytes of IgH-c-myc transgenic mice were compared with wild-type animals. Experiments were performed in duplicate (each sample consisted of RNA from 3 mice). RNA from lymphoma cells (purified with B220-coupled beads from Miltenyi Biotech) isolated from IgH-c-myc mice was also analyzed by. microarray (Nice-Sophia Antipolis Microarray Facility).[23,24] Quantification of normalized gene expression (transcripts per million [TPM]) was obtained from raw RNAseq data, using Kallisto.[25] Principal component analysis (PCA) and hierarchical clustering (Ward-Pearson) were performed, respectively, with Easy Microarray Analysis and edgeR R packages, using Kallisto TPM tables. Genes with low expression (TPM $<$ 4 for $<$ 4 samples), non-protein-coding genes, genes on sex chromosomes, and gene model genes were removed from TPM tables. Differential analysis was performed with Sleuth.[25] Gene set enrichment analysis (GSEA) was used to evaluate enriched molecular signatures (either gene ontology (GO) biological processes or BL signatures from Hummel et al[26] and Sha et al[27]). RNAseq data were deposited in the Gene Expression Omnibus database with accession number GSE132721.

Flow cytometry analysis

Single-cell suspensions of lymphomas from spleen and/or lymph nodes were labeled with various antibodies: anti-B220-BV510 (BioLegend), anti-CD19-PE (e-Bioscience), anti-CD117-BV421 (BD Biosciences), anti-IgM-fluorescein isothiocyanate (e-Bioscience), anti-IgD-BV421 (BioLegend), anti-CD5-fluorescein isothiocyanate (BD Biosciences), anti-CD138-APC (BD Biosciences), anti-CD4-PE (BD Biosciences), anti-CD8-PC5 (BD Biosciences), anti-CD11b-APC-eF780 (e-Bioscience), and anti-CD43-PE (BD Biosciences). Cells were analyzed on a Fortessa LSR2 (Beckman Coulter, Fullerton, CA).

Results

The location of c-myc in the IgH locus for the 3 transgenic models (c-myc-KIE$_\mu$, c-myc-KIC$_\mu$, and c-myc-KIC$_\alpha$) is schematized in Figure 1A.

B-cell expression of c-myc in young IgH-c-myc transgenic mice

We first used real-time PCR to analyze tissue c-myc RNA expression in 6- to 8-week-old IgH-c-myc transgenic mice. At this point, premalignant mice showed markedly elevated levels of c-myc transcripts in B-cell splenocytes compared with controls (Figure 1B). In agreement with data reporting that at the mature B-cell stage, IgH transcription is totally under the 3′RR control[28]; no differences were documented among the 3 c-myc models. c-myc transcripts were also markedly elevated in femoral bone marrow immature B cells of transgenic mice compared with controls (Figure 1B). Because at the immature B-cell stage IgH transcription is under both E$_\mu$ and 3′RR control,[29] c-myc transcription in c-myc-KIE$_\mu$ mice was significantly elevated compared with c-myc-KIC$_\mu$ mice (devoid of the E$_\mu$ enhancer) and c-myc-KIC$_\alpha$ mice (with a c-myc inserted in a position that is only accessible at late stages of B-cell maturation). The overexpression of B-cell c-myc transcripts translated into elevated levels of B-cell c-myc protein (Figure 1C).

B-cell proliferation and apoptosis in young IgH-c-myc transgenic mice

As reported in Figure 1D, proliferation of B-cell splenocytes from transgenic mice was significantly elevated in response to low doses of anti-CD40 plus LPS compared with *wt* B cells. The rate of H_2O_2-induced apoptosis was also significantly higher in transgenic B-cell splenocytes compared with *wt* B cells (Figure 1D). Thus, premalignant splenic B cells from IgH-c-myc mice showed increased proliferation and apoptosis compared with *wt* B cells, but with no differences between the 3 transgenic models.

Lifespan of IgH-c-myc transgenic mice

Beginning at age 4 months, transgenic mice progressively developed profound enlargement of lymph nodes (inguinal/brachial, superficial/deep cervical, mediastinal, and mesenteric) and spleens. Mice exhibiting obvious tumors or presenting signs of illness were sacrificed. Twenty-six c-myc-KIE$_\mu$, 21 c-myc-KIC$_\mu$, and 42 c-myc-KIC$_\alpha$ mice were followed to record their lifespan. The mean age of death for c-myc-KIE$_\mu$ transgenic mice was approximatively 6 months. Mean survival for c-myc-KIC$_\mu$ and c-myc-KIC$_\alpha$ transgenic mice was approximately 13 months (Figure 2A). Tumors in c-myc-KIE$_\mu$ mice appeared significantly sooner ($P < .0001$, Gehan-Breslow-Wilcoxon test) than in c-myc-KIC$_\mu$ and c-myc-KIC$_\alpha$ mice. The locations (spleen, mesenteric lymph nodes, inguinal/brachial lymph nodes, and mediastinal lymph nodes) of these B-cell lymphomas were similar in the 3 IgH-c-myc models (Figure 2B). The strong proliferative activity of these tumor cells was highlighted by high expression of the nuclear proliferation-associated antigen Ki67, a nuclear protein present during G$_1$, S, G$_2$, and M phases of the cell cycle. In agreement with their kinetics of emergence, the Ki67 index was significantly elevated in c-myc-KIE$_\mu$ mice compared with c-myc-KIC$_\mu$ and c-myc-KIC$_\alpha$ mice (Figure 2C). PCR (with a forward primer in the V$_H$J558 family and a reverse 3′ to the J$_{H4}$ segment) on genomic B-cell lymphoma DNA revealed rearranged bands indicating lymphoma cells from clonal origins (Figure 2D). PCR on genomic DNA including various tissues (spleen, lymph nodes) from the same lymphoma mice revealed similar rearranged bands indicating that spleen and lymph nodes were invaded by lymphoma cells from the same clonal origin (data not shown). VDJ repertoire sequencing of B-cell lymphomas confirmed their clonal status (Figure 2E) and revealed no bias compared with the normal B-cell repertoire of healthy mice (Figure 2F). Thus, the insertion of c-myc in the IgH locus did not favor the proliferation of a specific B-cell subset such as those expressing an autoreactive BCR. Finally, Ig V$_H$ genes were sequenced in tumors. Strikingly, and as previously reported for other murine B-cell lymphomas,[30] all were essentially un-mutated (0.27 $\pm$ 0.08 vs 0.43 $\pm$ 0.08 mutations per 100 bp for *wt* splenic B cells and lymphoma B cells, respectively; $P = .82$, Mann-Whitney *U* test).

Phenotypic analysis of B-cell lymphomas in IgH-c-myc mice

Figure 3A reports typical flow cytometry analysis (B220, CD19, CD43, CD117, CD138, IgM, IgD) for lymphoma phenotyping. All lymphomas obviously have a B-cell phenotype assessed by the presence of either B220 or CD19 B-cell surface antigens and the absence of CD4/CD8 T-cell antigens and CD11b monocyte antigen (supplemental Table 2). Only 2 among 89 B-cell lymphomas expressed CD5, which assigned their B2 (but not B1) phenotype.

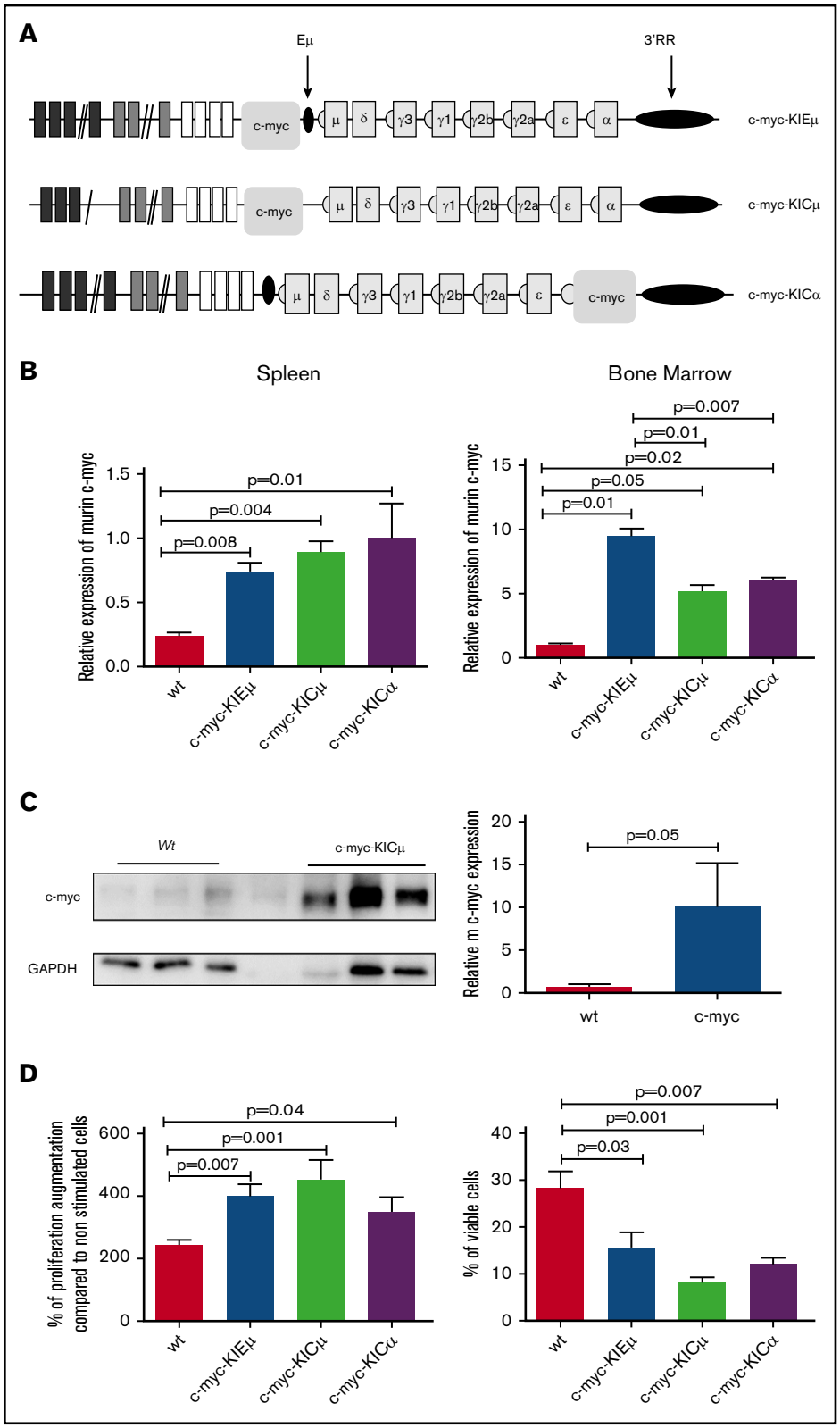

Figure 1. c-myc in IgH-c-myc transgenic mice. (A) Schematic representation of the IgH locus (not to scale) with the location of the inserted c-myc. (B) QPCR analysis of c-myc transcripts in B-cell splenocytes (left) and immature bone marrow B-cells (right). B-cell splenocytes results are reported as means ± standard error of the mean (SEM) of 4 c-myc-KIE$_\mu$, 5 c-myc-KIC$_\mu$, 3 c-myc-KIC$_\alpha$, and 8 *wt* mice. Immature bone marrow B-cell results are reported as means ± SEM of 5 c-myc-KIE$_\mu$, 3 c-myc-KIC$_\mu$, 4 c-myc-KIC$_\alpha$, and 3 *wt* mice. Significances were determined with the Mann-Whitney *U* test. (C) Western blot analysis of c-myc in B-cell splenocytes from *wt* and transgenic mice. An experiment with cells from 3 *wt* mice and 3 c-myc-KIC$_\mu$ mice is reported. Significance determined with the Mann-Whitney *U* test. Please note that line 4 contains a too-diluted c-myc sample not included in the statistical analysis (this line was kept to conserve the original format of the western blot). The original blot is reported in supplemental Figure 1. (D) Proliferation (left) and apoptosis (right) in B splenocytes from IgH c-myc KI transgenic mice. (Left) Proliferation was evaluated with the 3-(4,5 dimethylthiazol-2-yl)-5-(3-carboxymethoxyphenyl-2-(4-sulfophenyl)-2H-tetrazolium assay after 3 days stimulation with 0.5 μg/mL LPS + 0.1 μg/mL anti-CD40. Results (percentage of increase compared with unstimulated cells) are reported as means ± SEM of 4 c-myc-KIE$_\mu$, 8 c-myc-KIC$_\mu$, 7 c-myc-KIC$_\alpha$, and 18 *wt* mice. (Right) Apoptosis in B-cell splenocytes from IgH c-myc KI transgenic mice. Percentages of living cells were determined after 24 hours treatment with 0.01 μM H_2O_2. Results are reported as means ± SEM of 4 c-myc-KIE$_\mu$, 6 c-myc-KIC$_\mu$, 6 c-myc-KIC$_\alpha$, and 14 *wt* mice.

Flow cytometry analysis revealed a majority of mature B-cell lymphomas (IgM$^+$IgD$^+$) for the 3 IgH-c-myc models (Figure 3B). If the ratio of mature (IgM$^+$IgD$^+$)/immature (IgM$^+$IgD$^-$) B-cell lymphomas was similar between these mice, an elevated percentage of plasmablastic CD138$^+$ lymphomas was found for c-myc-KIE$_\mu$ mice (Figure 3C). Strikingly, an elevated percentage of B-cell lymphomas with the loss of CD19 expression was found for c-myc-KIC$_\mu$ mice (Figure 3D).

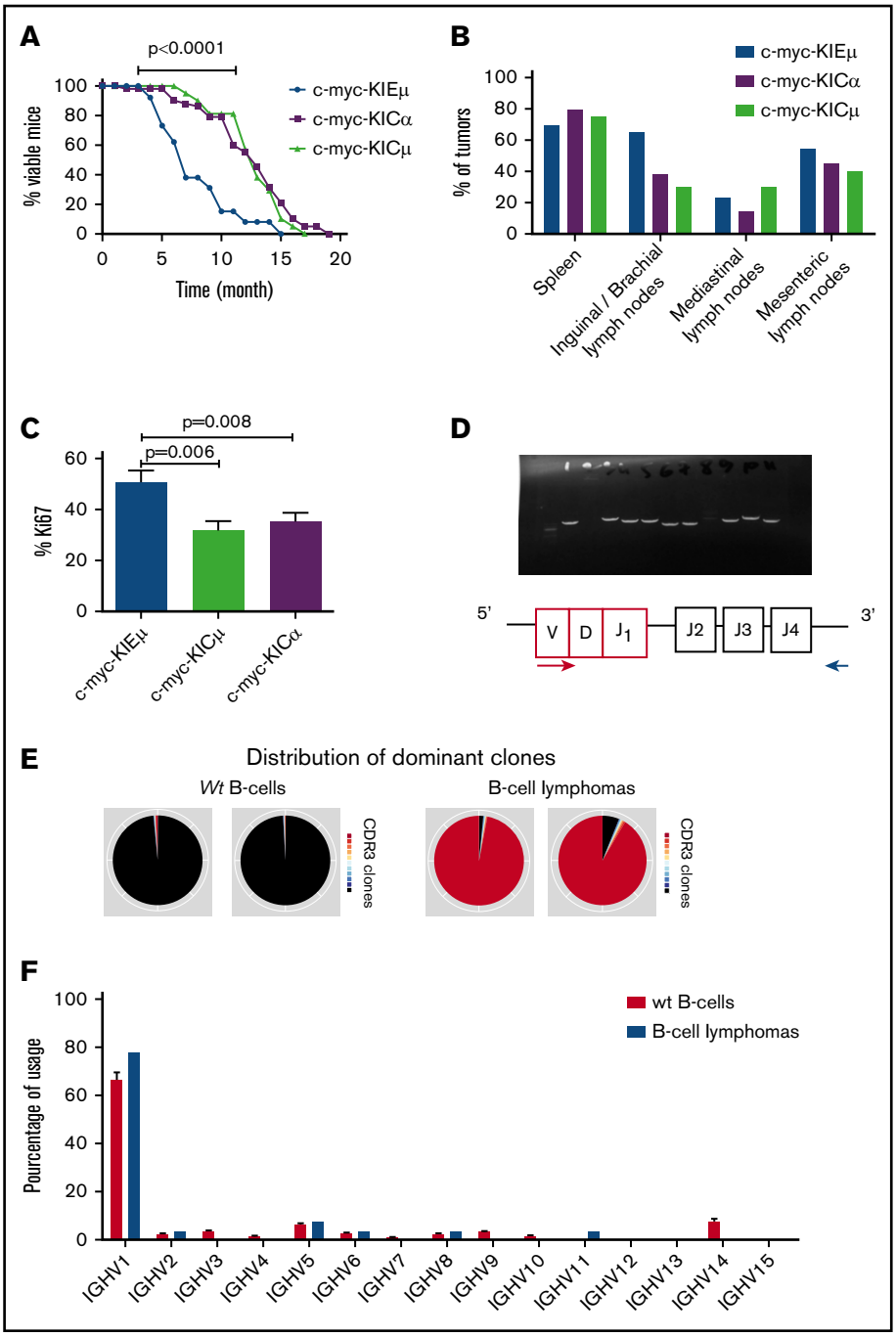

Figure 2. Lifespan of IgH-c-myc transgenic mice. (A) Survival curves of 26 c-myc-KIE$_\mu$, 21 c-myc-KIC$_\mu$, and 42 c-myc-KIC$_\alpha$ mice. Significance was determined with the Gehan-Breslow-Wilcoxon test. (B) Locations of lymphomas in c-myc-KIE$_\mu$, c-myc-KIC$_\mu$, and c-myc-KIC$_\alpha$ mice. Several sites were found in the same mouse. (C) Ki67 index of proliferation of B-cell lymphomas in IgH-c-myc transgenic mice. The Ki67 index was calculated in B-cell lymphomas from 24 c-myc-KIE$_\mu$, 20 c-myc-KIC$_\mu$, and 42 c-myc-KIC$_\alpha$ mice. (D) Clonal origin of B-cell lymphomas of IgH-c-myc transgenic mice. The forward primer was consensus for the V$_H$J$_{558}$ family and the reverse primer was 3′ to the J$_{H4}$ segment, thus amplifying in theory 4 rearranged bands (V$_H$J558D$_x$J$_1$, V$_H$J558D$_x$J$_2$, V$_H$J558D$_x$J$_3$, and V$_H$J558D$_x$J$_4$) of various lengths. The scheme represents a VDJ$_1$ rearrangement. Amplification with several different genomic DNAs confirmed the clonal status of the B-cell lymphoma. The lack of amplification indicated the use of a V segment different from the V$_H$J558 family. The size marker is in the first lane. (E) Sequencing confirmed the clonal status of B-cell lymphoma of IgH-c-myc transgenic mice. Two representative experiments of 5 for *wt* mice (left) and of 27 for B-cell lymphomas from IgH-c-myc transgenic mice (right) are reported. (F) The V$_H$ segments used for B-cell lymphomas from IgH-c-myc transgenic mice matched with the B-cell repertoire in *wt* mice (same mice as in panel E).

Transcriptome analysis of nonmalignant and malignant B cells

To document molecular signatures of tumors in the 3 IgH-c-myc transgenic models, RNA sequencing of 28 B-cell samples (B220$^+$ IgM$^+$IgD$^+$) was performed, and normalized expression data were obtained for all protein-coding genes. In Figure 4A-B, PCA and hierarchical clustering clearly defined groups of samples with similar transcriptome signatures. Nonmalignant (resting and LPS-stimulated) B-cell samples appear as distinct clusters from tumor samples. These samples segregate as 2 distinct groups (of, respectively, 6 and 13 samples) both in PCA and hierarchical clustering representations. We thus define group I as the 6-sample cluster that shares more similarities with LPS-stimulated B-cell samples and group II as the other 13-sample cluster. Among 20 tumor samples, 4 CD138$^+$ samples are found only in group II. Of note, 1 c-myc-KIE$_\mu$ sample did not cluster in either of these 2 groups and was withdrawn from further differential analysis. Nonmalignant B-cell samples not only provide reference data to attest to the transcriptome signature of tumor samples but also identify differences in gene expression, depending on the c-myc insertion. Figure 4C exhibits gene expression and hierarchical clustering of the top 100 most variable genes across 8 nonmalignant B-cell samples. Again, independent of the c-myc insertion

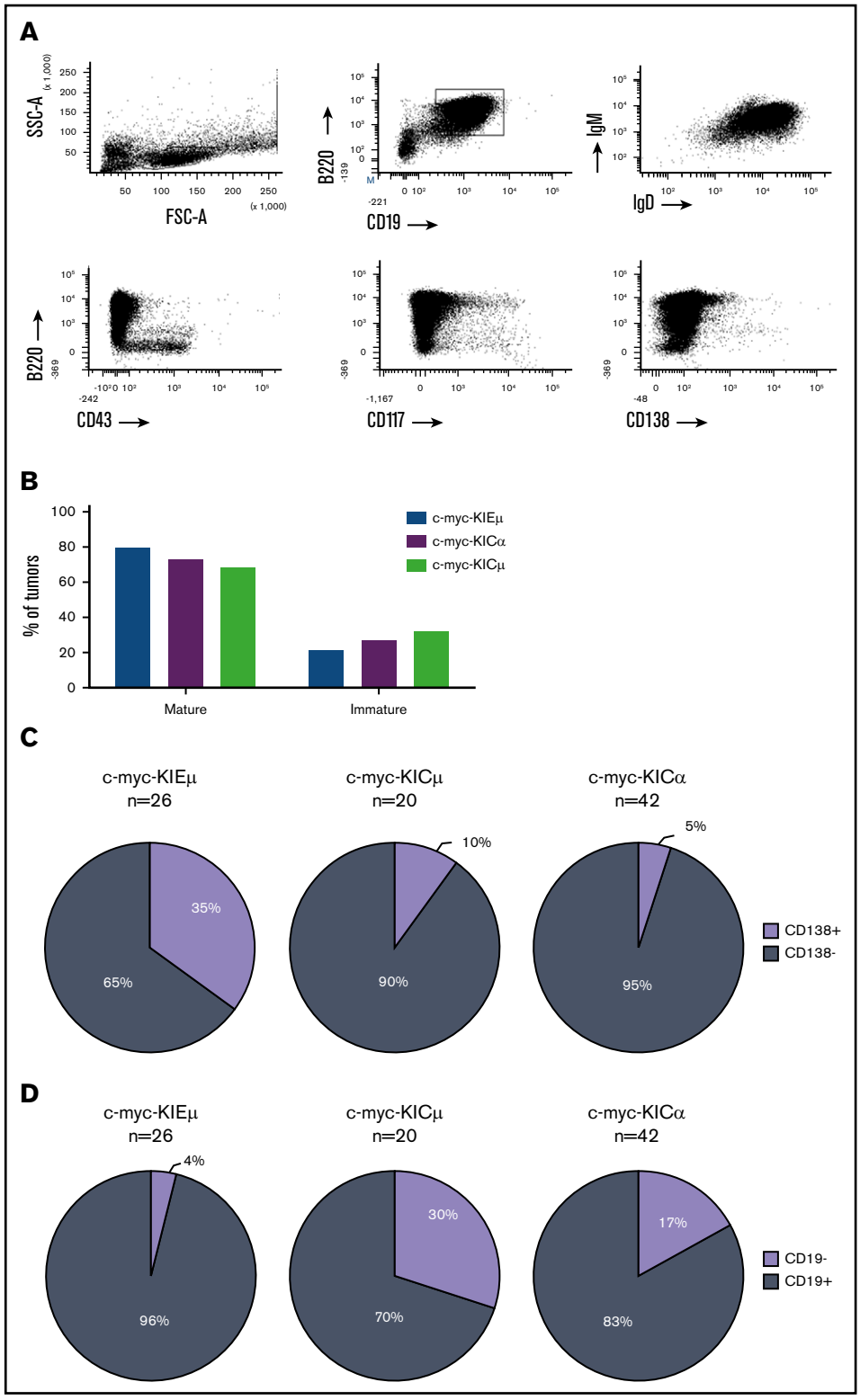

Figure 3. B-cell lymphoma phenotypes in IgH-c-myc transgenic mice. (A) A typical flow cytometry analysis for B-cell lymphoma phenotyping. One representative experiment for a B220^{+}CD19^{+}IgM^{+}IgD^{+}CD43^{-}CD117^{-}CD138^{-} B-cell lymphoma is shown. (B) Percentage of mature (IgM^{+}IgD^{+}) and immature (IgM$^{+/-}$IgD^{-}) B-cell lymphomas (24 c-myc-KIE$_{\mu}$, 19 c-myc-KIC$_{\mu}$, and 37 c-myc-KIC$_{\alpha}$ mice). (C) Percentages of CD138^{+} mature B-cell lymphomas in c-myc-KIE$_{\mu}$, c-myc-KIC$_{\mu}$, and c-myc-KIC$_{\alpha}$ mice. The number (n) of mice for each group is indicated. (D) Percentages of CD19^{-} mature B-cell lymphomas in c-myc-KIE$_{\mu}$, c-myc-KIC$_{\mu}$, and c-myc-KIC$_{\alpha}$ mice. Same mice as in panel C.

site, all 3 models share a common B-cell signature with the *wt* control, under both resting and LPS-stimulated conditions. Figure 4D shows expression data for 4 representative B-cell activation genes (*AICDA*, *EXOSC3*, *CCR6*, *CDH17*), emphasizing similar gene regulation of relevant biological processes. Functional profiling of tumor samples was achieved by analyzing differential gene expression between the 2 above-defined groups (group II vs group I; Figure 5A). Among 9995 genes that passed the minimum-expression filter, 2236 genes exhibit significantly different expression (adjusted $P < .05$), most of them with slight to moderate differences. Limiting to genes changing

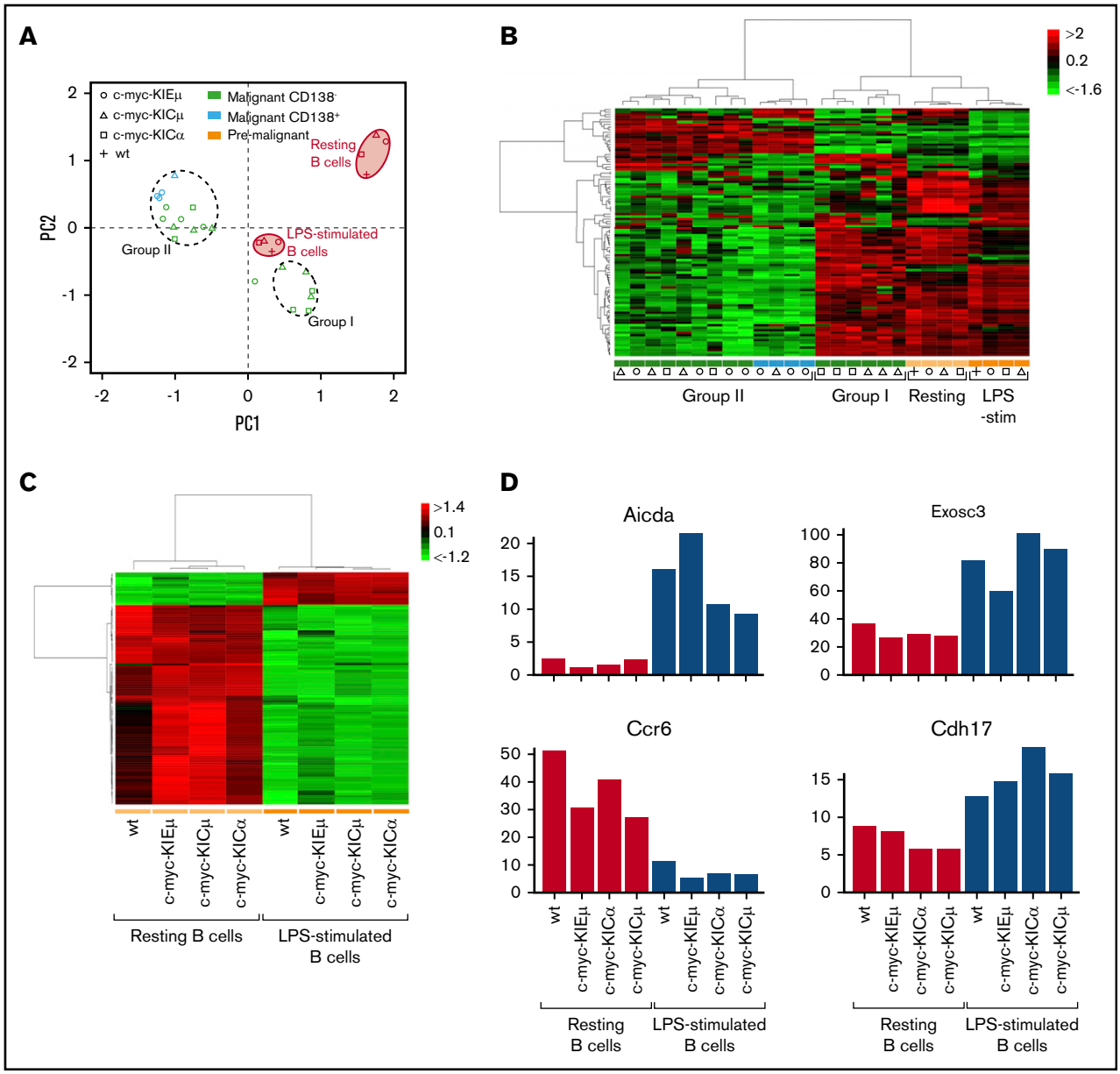

Figure 4. RNAseq analysis of splenic B cells and B-cell lymphomas. (A) PCA of RNAseq gene expression data from 1 *wt* splenic B-cell sample (stimulated or not with LPS), 3 premalignant B-cell samples (stimulated or not with LPS) and 20 tumor samples. Each *wt* and premalignant B-cell sample is pooled mRNA from 4 different mice. Same mice for LPS-stimulated and unstimulated B cells. Premalignant splenic B-cell samples were from c-myc-KIE$_\mu$, c-myc-KIC$_\mu$, and c-myc-KIC$_\alpha$ mice. (B) Heat map of the 100 most variable gene expressions across all samples; hierarchical clustering of genes per sample according to Pearson's correlation metric and Ward's method. Same symbols, colors, and group definitions as in panel A. (C) Heat map of 100 most variable gene expressions across the *wt* and premalignant B-cell samples only; hierarchical clustering of genes per sample according to Pearson's correlation metric and Ward's method. (D) Expression of 4 representative genes (drawn from GO:0002312 "B-cell activation involved in immune response") in *wt* and premalignant samples. AICDA, gene for the AID protein implicated in Ig somatic hypermutation and CSR; CDH17, a member of the cadherin superfamily; CCR6, the MIP-3α receptor; EXOSC3, subunit of the RNA exosome.

by more than 2-fold, we found 225 upregulated genes and 588 downregulated genes in group II compared with in group I samples (>4-fold: 68 up genes, 231 down genes). The set of differentially expressed genes indeed segregates samples according to expected groups, as emphasized in Figure 5B. GSEA software identified upregulated biological processes (as defined in gene ontology) in each group (Figure 5C). Distribution of genotypes according the group I and group II classifications showed a significant commitment of c-myc-KIE$_\mu$ samples to group II (Figure 5C). Group I tumor samples revealed a prevalence of immune regulation pathways, as one would expect from the proximity of their transcriptomic profiles to those of activated B cells (Figure 4A-B). Group II tumor samples were characterized by enriched DNA metabolism and cell cycle pathways, indicative of proliferative disorders. More specifically, enrichment of previously established[27] human BL signatures was tested in group II

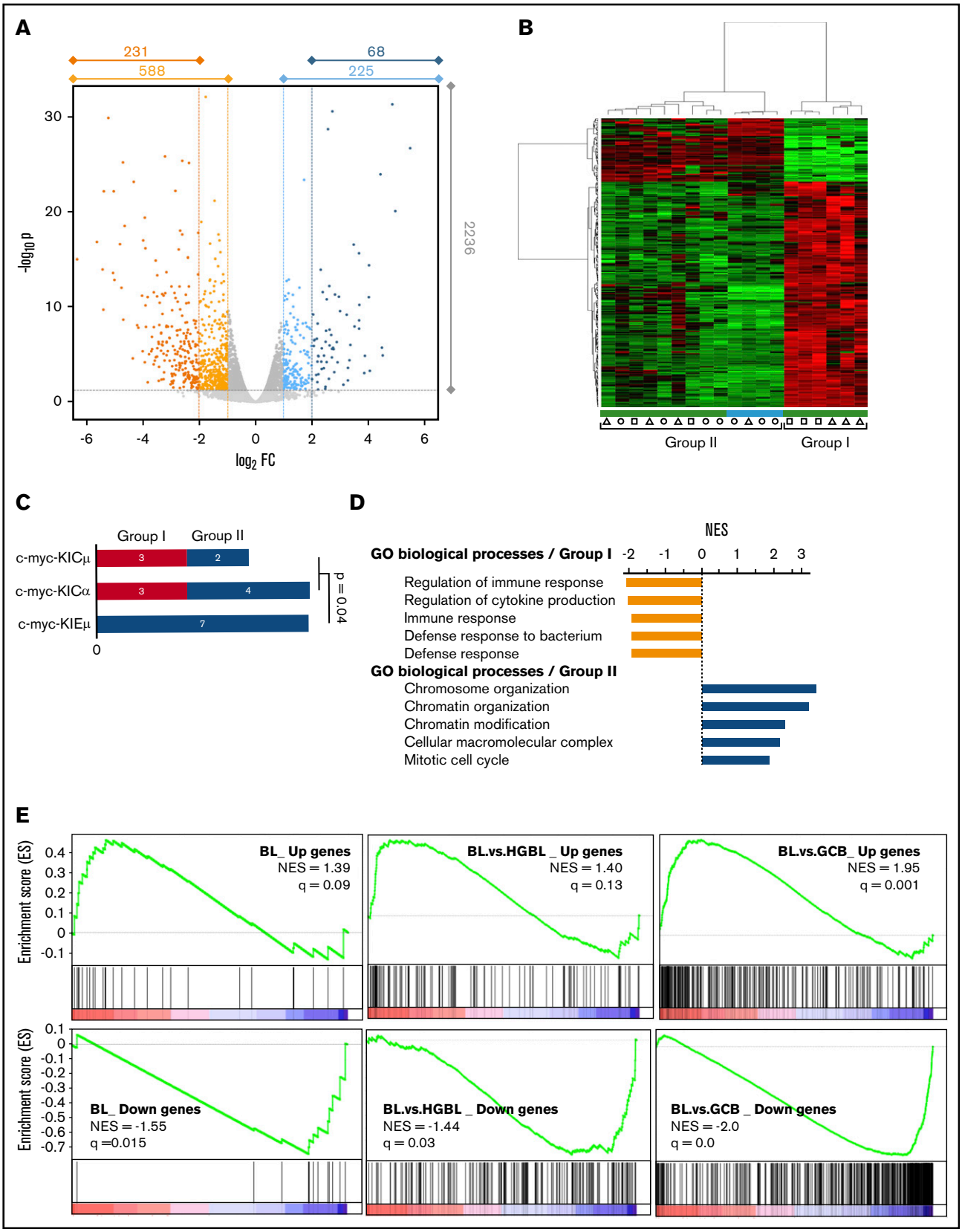

Figure 5. Analysis of B-cell lymphomas in transgenic mice. (A) Volcano plot of differential gene expression in group II vs group I tumor samples. Same B-cell lymphomas as in Figure 4A. The numbers of significantly upregulated (in blue) and downregulated (in orange) genes are shown. (B) Heat map of the 100 most variable gene expressions across all tumor samples; hierarchical clustering of genes/samples according to Pearson's correlation metric and Ward's method. Same symbols, colors, and group definitions

vs group I differential expression results. All BL up and down signatures were significantly enriched at false discovery rate q < 25%, emphasizing the molecular similarity of group II tumor samples to human BL cells (Figure 5E, left). Moreover, from normalized enrichment scores and q-values, group II vs group I differential expression was closer to the BL vs DLBCL (diffuse large B-cell lymphoma) signature (Figure 5E, medium) than it was to the BL vs high-grade B-cell lymphoma signature (Figure 5E, right), indicating molecular similarity of group I tumor samples to DLBCL.

Discussion

c-myc translocation in the IgH locus followed by its deregulation seems to be the key step in BL development. Consistent with this critical role of c-myc, mouse models carrying insertions of c-myc into the IgH locus develop B-cell and plasma cell neoplasms.[19-21] However, the precise role of IgH *cis*-transcriptional enhancers on c-myc deregulation in the context of the IgH locus remains an open question. Analysis of mice bearing c-myc insertion into 3 different sites in the IgH locus showed the additive contribution of both E_μ and 3′RR *cis*-enhancers in c-myc deregulation. In agreement with the pro-B to immature B-cell window of activity of E_μ,[31,32] E_μ is a c-myc deregulator during the immature steps of B-cell lymphopoiesis. In agreement with its pre-B to mature B-cell window of activity,[29,31] the 3′RR deregulates c-myc from the immature to the mature steps of B-cell lymphopoiesis. When both E_μ and 3′RR are present in the IgH locus, c-myc deregulation occurs during all stages of B-cell maturation, as previously reported with an E_μ-GFP-3′RR transgene.[33]

E_μ has been used to deregulate c-myc with the aim of mimicking human BL, but E_μ-c-myc transgenic mice developed malignancies with a pro-B phenotype rather than the IgM^+IgD^+ mature phenotype observed in BL.[6] The c-myc KI into the IgH locus did not generate B-cell malignancies with a pro-B phenotype suggesting that the physiological window of activity of E_μ during B-cell maturation (pro-B/pre-B-cell stages) is insufficient by itself to initiate their development. However, the absence of E_μ (c-myc-KIC_μ mice) or c-myc insertion into the constant heavy chain region (c-myc-KIC_α mice) where E_μ has no transcriptional role[28] markedly delays the rate of B-cell lymphoma occurrence. These results clearly show a contribution (although nonessential) for E_μ in B-cell lymphomagenesis. The ability of E_μ alone, that is, in an IgH locus devoid of a 3′RR, to induce B-cell lymphomagenesis remains an open question. The physiological rationale of such mice for human B-cell lymphomagenesis would be doubtful, as the 3′RR is always conserved after oncogene translocation into the IgH locus. At this time, the development of c-myc-induced plasmacytomas in mice bearing a truncated 3′RR gave divergent results.[34,35]

Insertion of c-myc into the IgH locus displayed an increase in c-myc transcripts in B cells of young mice. In most cell types, c-myc enforces proliferation but also triggers apoptosis. We demonstrated such an effect in B splenocytes from young transgenic mice. No differences were found with respect to the location of the inserted c-myc. This result reinforces data reporting that in mature B cells, the IgH locus falls totally under the transcriptional control of the 3′RR.[28] Confirming these data, RNAseq analysis of resting and LPS stimulated B cells from transgenic mice did not reveal specific signatures between them. Furthermore, their transcriptome signatures in response to LPS stimulation were similar to those of *wt* B cells indicating that IgH c-myc insertion by itself is not sufficient to dramatically affect B-cell physiology. These results confirm the concept that if c-myc translocation into the IgH locus is the *primum movens* of B-cell lymphomagenesis, it is the progressive accumulation of mutations (affecting cell proliferation, apoptosis, differentiation, and metabolism) generated by the c-myc-induced genomic instability that plays the critical role in B-cell lymphoma emergence.

c-myc insertion in front of E_μ or in front of C_μ (with E_μ deletion) prevents the development of efficient VDJ recombination and BCR expression by this chromosome. It is the other chromosome carrying an intact IgH locus that will be used for B-cell development. Insertion of c-myc in front of the 3′RR (into C_α) does not prevent VDJ recombination, BCR expression, and B-cell development. During B-cell maturation, IgH loci of both chromosomes were transcribed and underwent CSR. A 3-dimensional chromatin loop bringing E_μ and 3′RR into close proximity is found in resting B cells and during CSR.[18] Could c-myc KI between the enhancers disrupt their cooperation, explaining that deleted E_μ and mice with c-myc KI close to the 3′RR enhancer have a similar c-myc expression pattern, tumor localization, and life expectancy? This seems unlikely because no transcriptional cooperation has been documented between E_μ and 3′RR enhancers at mature[28] and immature B-cell stages.[13] Moreover, deletion of the E_μ enhancer did not affect CSR and DNA repair.[36] Are these E_μ-3′RR IgH intrachromosomal interactions really relevant? We favor the hypothesis that they are only mechanical because of the IgH location of both E_μ and 3′RR and to 3-dimensional folding bringing switch regions into contact with each other. The simplest explanation is an additive effect of E_μ and 3′RR on c-myc transcription during B-cell maturation. E_μ deletion is thus equivalent to the c-myc KI close to the 3′RR, as E_μ has no transcriptional effect on transcription of IgH constant genes at immature and mature B-cell stages.[13,28]

5′E_μ and/or 3′RR oncogene-induced deregulations had no influence on the localization of B-cell lymphomas and a minor effect on their degree of maturity and phenotypic characteristics (an elevated percentage of $CD138^+$ lymphoma for c-myc-KIE_μ mice was, however, found). Two specific transcriptome signatures were detected for mature (IgM^+IgD^+) B-cell lymphomas from c-myc-KIE_μ, c-myc-KIC_μ, and c-myc-KIC_α mice. One is clearly a signature that mimics that of human BL, which does not or only slightly resembles that of LPS-activated B cells (such as those in indolent B-cell lymphomas). These results reinforce the concept that regardless of the location of the IgH c-myc insertion, it is the progressive accumulation of mutations generated by c-myc-induced genomic instability that participate in B-cell lymphoma

Figure 5. (continued) as in Figure 4A. (C) Number of RNAseq samples in each group according to genotype. *P* value from Fisher's exact test. (D) Summary of GSEA analysis of differential gene expression: top 5 enriched GO biological processes (false discovery rate <0.05, size >80) for both groups. (E) Detailed GSEA analysis of differentially expressed genes against human BL signatures (up- and downregulated genes from Hummel et al[26] [left] and from Sha et al[27] [middle and right]) defined by BL vs germinal center (GC) B-cell like DLBCL (left), BL vs HGBVL (middle), or BL vs GC-DLBCL (right) comparisons.

emergence. The emergence of B-cell lymphomas was significantly elevated when c-myc was under the transcriptional control of both 5′ and 3′ IgH enhancers (schematized with c-myc-KIE$_\mu$ mice). This is the first report of their in vivo transcriptional cooperation for oncogene deregulation in the context of the endogenous IgH locus. Previous studies have highlighted such transcriptional cooperation with transgenic models bearing a GFP cassette.[29,32,33] The most notable difference for c-myc-KIE$_\mu$ mice compared with c-myc-KIC$_\mu$ and c-myc-KIC$_\alpha$ mice is their elevated amounts of c-myc transcripts at immature B-cell stages when c-myc transcription is still under the transcriptional control of the E$_\mu$ enhancer. The most important effect of E$_\mu$ and 3′RR cooperation in c-myc deregulation is their higher rate of B-cell lymphoma emergence that fits well with their higher Ki67 proliferation index compared with B-cell lymphomas in mice without E$_\mu$ or with c-myc inserted into C$_\alpha$. Transcriptome analysis of B-cell lymphomas in c-myc-IgH transgenic mice highlighted the prevalence of proliferative pathways instead of alterations in apoptotic programs for their development. Similar results were reported with c-myc-3′RR transgenic animal,[16,17,24] when more than half of the lymphomas arising in E$_\mu$-myc mice,[37] or after insertion of truncated 3′IgH upstream of the c-myc coding region,[15] overexpressed the anti-apoptotic molecules Bcl-2 and Bcl-xL.

If the vast majority of B-cell lymphomas expressed CD19, a specific subset of CD19$^-$ B-cell lymphomas was found for c-myc-KIC$_\mu$ mice. CD19 is a B-cell-specific membrane protein regulating BCR-independent and BCR-dependent signal transduction pathways. Loss of CD19 reduced lymphomagenesis in c-Myc-E$_\mu$ transgenic mice showing that a c-myc:CD19 regulatory loops positively controls B-cell lymphoma progression.[38] However CD19 deficiency was reported to aggravate the antitumor immune response by affecting T-cell activation.[39] CD19 loss was also associated with poorer survival in patients with diffuse large B-cell lymphoma.[40] Thus, in some cases, CD19 deficiency may be used by the B-cell lymphoma for its progression and development. Why a specific subset of B-cell lymphomas developed only in an E$_\mu$-deficient locus remains an open question.

Our study primarily examines the contribution of E$_\mu$ and/or 3′RR IgH enhancers to c-myc deregulation and B-cell lymphomagenesis. However, it also is relevant concerning different types of myc rearrangements encountered in different human B-cell lymphomas. c-myc rearrangement not only is characteristic of BL but is also found in high-grade B-cell lymphoma (in association with bcl2 and/or bcl6 rearrangements), DLBCL (both not otherwise specified or germinal center B-cell type), in plasmablastic lymphoma, unclassifiable B-cell lymphoma with intermediate features between DLBCL and BL (B-UNC/BL/DLBCL), and myeloma.[41-44] Comparison of transcriptome analyses indicated that group II tumor samples had strong similarities to human BL, whereas group I tumor samples were closer to DLBCL. These results reinforce the suitability of IgH-c-myc mice as a model to study human B-cell lymphomas with c-myc translocation to the IgH locus.

In summary, we have shown with the synchronous usage of 3 transgenic mice models, the additive cooperation of the 2 IgH transcriptional enhancers Eμ and 3′RR in c-myc deregulation leading to B-cell lymphomagenesis. We also assessed the predominant contribution of the 3′RR transcriptional element to mature B-cell lymphoma generation. This result is in agreement with the long-distance effect of 3′RR on IgH transcription at mature B-cell stages.[28] Indeed, during B-cell development, the 3′RR is crucial for μ chain transcription and density of BCR expression at the B-cell membrane.[7] 3′RR knock-out models indicate that its deletion affects mature B-cell lymphoma occurrence, highlighting the key role of this IgH *cis*-regulatory region for lymphoma progression.[34,35,45] Therefore, as previously reported by us and others,[3,35,46] 3′RR targeting would in theory provide a potential strategy for the treatment of mature B-cell lymphomas. Translocations in B-cell lymphomas induce epigenetic changes,[47] suggesting that epigenetic drugs that target histone acetylation (inhibitors of histone deacetylases) and histone methylation (EZH2 inhibitors) may provide a new strategy to treat several B-cell lymphoid malignancies.[48] Recently, data demonstrated that direct inhibition of EZH2 and histone deacetylases are synergistic in germinal center B-cell lymphomas.[49] Reports have documented that 3′RR activation and transcription can be downregulated by inhibitors of histone deacetylases.[50] 3′RR-induced effects are largely mediated through activation of specific epigenetic marks in 3′RR targeted DNA,[8] reinforcing the idea that targeting the IgH 3′RR would be of interest in the downregulation of oncogene transcription. Furthermore, data obtained from mice are transferable to human lymphomagenesis with respect to the strong structural homology between mouse and human 3′RRs.[51] Altogether, these results reinforce the hypothesis that considers 3′RR as an interesting target for antilymphoma drug therapy.

Acknowledgments

The authors are “Equipe Labellisée LIGUE 2018.” This work is also supported by Agence Nationale de la Recherche (ANR) “Epi-Switch 2016.” N.G. is supported by a grant from “Société Française d’Hématologie” and ANR “Epi-Switch 2016.” H.I. is supported by University of Limoges (France) and ANR “Epi-Switch 2016.” M.F. is supported by “Région Nouvelle Aquitaine” (France). F.B. is supported by Fondation Partenariale de l’Université de Limoges and Association Limousine pour l’Utilisation du Rein Artificiel à Domicile.

Authorship

Contribution: N.G., H.I., M.F., and C.C. performed flow cytometry experiments and analysis; N.G., H.I., M.F., and Y.D. performed research; J.C.-M. and Y.D. designed research; Y.D. and F.B. analyzed mRNAseq data; N.G., H.I., M.F., F.B., C.C., J.C.-M., and Y.D. wrote the paper; and Y.D. obtained grant support.

Conflict-of-interest disclosure: The authors declare no competing financial interests.

ORCID profiles: C.C., 0000-0003-3221-6319; Y.D., 0000-0003-0143-5543; F.B., 0000-0002-0351-685X.

Correspondence: Yves Denizot, UMR CNRS 7276, Inserm U1262, CBRS, Rue du Professeur Descottes, 87025 Limoges, France; e-mail: yves.denizot@unilim.fr; and François Boyer, UMR CNRS 7276, Inserm U1262, CBRS, Rue du Professeur Descottes, 87025 Limoges, France; e-mail: francois.boyer@unilim.fr.

References

1. Blum KA, Lozanski G, Byrd JC. Adult Burkitt leukemia and lymphoma. *Blood*. 2004;104(10):3009-3020.
2. Kuzyk A, Mai S. c-MYC-induced genomic instability. *Cold Spring Harb Perspect Med*. 2014;4(4):a014373.
3. Ghazzaui N, Saintamand A, Issaoui H, Vincent-Fabert C, Denizot Y. The IgH 3′ regulatory region and c-myc-induced B-cell lymphomagenesis. *Oncotarget*. 2017;8(4):7059-7067.
4. Perlot T, Alt FW, Bassing CH, Suh H, Pinaud E. Elucidation of IgH intronic enhancer functions via germ-line deletion. *Proc Natl Acad Sci USA*. 2005; 102(40):14362-14367.
5. Marquet M, Garot A, Bender S, et al. The Eμ enhancer region influences H chain expression and B cell fate without impacting IgVH repertoire and immune response in vivo. *J Immunol*. 2014;193(3):1171-1183.
6. Adams JM, Harris AW, Pinkert CA, et al. The c-myc oncogene driven by immunoglobulin enhancers induces lymphoid malignancy in transgenic mice. *Nature*. 1985;318(6046):533-538.
7. Saintamand A, Rouaud P, Garot A, et al. The IgH 3′ regulatory region governs μ chain transcription in mature B lymphocytes and the B cell fate. *Oncotarget*. 2015;6(7):4845-4852.
8. Saintamand A, Rouaud P, Saad F, Rios G, Cogné M, Denizot Y. Elucidation of IgH 3′ region regulatory role during class switch recombination via germline deletion. *Nat Commun*. 2015;6(1):7084.
9. Rouaud P, Saintamand A, Saad F, et al. Elucidation of the enigmatic IgD class-switch recombination via germline deletion of the IgH 3′ regulatory region. *J Exp Med*. 2014;211(5):975-985.
10. Péron S, Laffleur B, Denis-Lagache N, et al. AID-driven deletion causes immunoglobulin heavy chain locus suicide recombination in B cells. *Science*. 2012;336(6083):931-934.
11. Rouaud P, Vincent-Fabert C, Saintamand A, et al. The IgH 3′ regulatory region controls somatic hypermutation in germinal center B cells. *J Exp Med*. 2013;210(8):1501-1507.
12. Rouaud P, Vincent-Fabert C, Fiancette R, Cogné M, Pinaud E, Denizot Y. Enhancers located in heavy chain regulatory region (hs3a, hs1,2, hs3b, and hs4) are dispensable for diversity of VDJ recombination. *J Biol Chem*. 2012;287(11):8356-8360.
13. Ghazzaui N, Issaoui H, Boyer F, Martin OA, Saintamand A, Denizot Y. 3'RR and 5'E_{μ} immunoglobulin heavy chain enhancers are independent engines of locus remodeling. *Cell Mol Immunol*. 2019;16(2):198-200.
14. Ghazzaui N, Issaoui H, Martin OA, et al. Trans-silencing effect of the 3'RR immunoglobulin heavy chain enhancer on Igκ transcription at the pro-B cell stage. *Cell Mol Immunol*. 2019;16(7):668-670.
15. Wang J, Boxer LM. Regulatory elements in the immunoglobulin heavy chain gene 3′-enhancers induce c-myc deregulation and lymphomagenesis in murine B cells. *J Biol Chem*. 2005;280(13):12766-12773.
16. Truffinet V, Pinaud E, Cogné N, et al. The 3′ IgH locus control region is sufficient to deregulate a c-myc transgene and promote mature B cell malignancies with a predominant Burkitt-like phenotype. *J Immunol*. 2007;179(9):6033-6042.
17. Rouaud P, Fiancette R, Vincent-Fabert C, et al. Mantle cell lymphoma-like lymphomas in c-myc-3'RR/p53+/- mice and c-myc-3'RR/Cdk4R24C mice: differential oncogenic mechanisms but similar cellular origin. *Oncotarget*. 2012;3(5):586-593.
18. Wuerffel R, Wang L, Grigera F, et al. S-S synapsis during class switch recombination is promoted by distantly located transcriptional elements and activation-induced deaminase. *Immunity*. 2007;27(5):711-722.
19. Rosean TR, Holman CJ, Tompkins VS, et al. KSHV-encoded vIL-6 collaborates with deregulated c-Myc to drive plasmablastic neoplasms in mice. *Blood Cancer J*. 2016;6(2):e398.
20. Park SS, Kim JS, Tessarollo L, et al. Insertion of c-Myc into Igh induces B-cell and plasma-cell neoplasms in mice. *Cancer Res*. 2005;65(4):1306-1315.
21. Cheung WC, Kim JS, Linden M, et al. Novel targeted deregulation of c-Myc cooperates with Bcl-X(L) to cause plasma cell neoplasms in mice. *J Clin Invest*. 2004;113(12):1763-1773.
22. Vincent-Fabert C, Saintamand A, David A, et al. Reproducing indolent B-cell lymphoma transformation with T-cell immunosuppression in LMP1/ CD40-expressing mice. *Cell Mol Immunol*. 2019;16(4):412-414.
23. Amin R, Marfak A, Pangault C, et al. The class-specific BCR tonic signal modulates lymphomagenesis in a c-myc deregulation transgenic model. *Oncotarget*. 2014;5(19):8995-9006.
24. Fiancette R, Rouaud P, Vincent-Fabert C, et al. A p53 defect sensitizes various stages of B cell development to lymphomagenesis in mice carrying an IgH 3′ regulatory region-driven c-myc transgene. *J Immunol*. 2011;187(11):5772-5782.
25. Bray NL, Pimentel H, Melsted P, Pachter L. Near-optimal probabilistic RNA-seq quantification [published correction appears in *Nat Biotechnol*. 2016; 34(8):888]. *Nat Biotechnol*. 2016;34(5):525-527.
26. Hummel M, Bentink S, Berger H, et al; Molecular Mechanisms in Malignant Lymphomas Network Project of the Deutsche Krebshilfe. A biologic definition of Burkitt's lymphoma from transcriptional and genomic profiling. *N Engl J Med*. 2006;354(23):2419-2430.
27. Sha C, Barrans S, Cucco F, et al. Molecular high-grade B-cell lymphoma: defining a poor-risk group that requires different approaches to therapy. *J Clin Oncol*. 2019;37(3):202-212.
28. Saintamand A, Vincent-Fabert C, Marquet M, et al. E_{μ} and 3'RR IgH enhancers show hierarchic unilateral dependence in mature B-cells. *Sci Rep*. 2017; 7(1):442.

29. Guglielmi L, Le Bert M, Truffinet V, Cogné M, Denizot Y. Insulators to improve expression of a 3(')IgH LCR-driven reporter gene in transgenic mouse models. *Biochem Biophys Res Commun*. 2003;307(3):466-471.

30. Saintamand A, Garot A, Saad F, Moulinas R, Denizot Y. Pre-germinal center origin for mature mouse B cell lymphomas: a major discrepancy with human mature lymphomas. *Cell Cycle*. 2015;14(22):3656-3658.

31. Pinaud E, Marquet M, Fiancette R, et al. The IgH locus 3′ regulatory region: pulling the strings from behind. *Adv Immunol*. 2011;110:27-70.

32. Guglielmi L, Truffinet V, Carrion C, et al. The 5'HS4 insulator element is an efficient tool to analyse the transient expression of an Em μ-GFP vector in a transgenic mouse model. *Transgenic Res*. 2005;14(4):361-364.

33. Guglielmi L, Le Bert M, Comte I, et al. Combination of 3′ and 5′ IgH regulatory elements mimics the B-specific endogenous expression pattern of IgH genes from pro-B cells to mature B cells in a transgenic mouse model. *Biochim Biophys Acta*. 2003;1642(3):181-190.

34. Kovalchuk AL, Sakai T, Qi CF, et al. 3′*Igh* enhancers hs3b/hs4 are dispensable for *Myc* deregulation in mouse plasmacytomas with T(12;15) translocations. *Oncotarget*. 2018;9(77):34528-34542.

35. Gostissa M, Yan CT, Bianco JM, Cogné M, Pinaud E, Alt FW. Long-range oncogenic activation of Igh-c-myc translocations by the Igh 3′ regulatory region. *Nature*. 2009;462(7274):803-807.

36. Issaoui H, Ghazzaui N, Ferrad M, Boyer F, Denizot Y. Class switch recombination junctions are not affected by the absence of the immunoglobulin heavy chain E_{μ} enhancer. *Cell Mol Immunol*. 2019;16(7):671-673.

37. Eischen CM, Woo D, Roussel MF, Cleveland JL. Apoptosis triggered by Myc-induced suppression of Bcl-X(L) or Bcl-2 is bypassed during lymphomagenesis. *Mol Cell Biol*. 2001;21(15):5063-5070.

38. Poe JC, Minard-Colin V, Kountikov EI, Haas KM, Tedder TF. A c-Myc and surface CD19 signaling amplification loop promotes B cell lymphoma development and progression in mice. *J Immunol*. 2012;189(5):2318-2325.

39. Ruella M, Maus MV. Catch me if you can: leukemia escape after CD19-directed T cell immunotherapies. *Comput Struct Biotechnol J*. 2016;14:357-362.

40. Kazantseva M, Hung NA, Mehta S, et al. Tumor protein 53 mutations are enriched in diffuse large B-cell lymphoma with irregular CD19 marker expression. *Sci Rep*. 2017;7(1):1566.

41. Beham-Schmid C. Aggressive lymphoma 2016: revision of the WHO classification. *Memo*. 2017;10(4):248-254.

42. Quintanilla-Martinez L. The 2016 updated WHO classification of lymphoid neoplasias. *Hematol Oncol*. 2017;35(suppl 1):37-45.

43. Xie Y, Pittaluga S, Jaffe ES. The histological classification of diffuse large B-cell lymphomas. *Semin Hematol*. 2015;52(2):57-66.

44. Misund K, Keane N, Stein CK, et al; MMRF CoMMpass Network. MYC dysregulation in the progression of multiple myeloma [published online ahead of print 22 August 2019]. *Leukemia*.

45. Saad F, Saintamand A, Cogné M, Denizot Y. The IgH 3′ regulatory region influences lymphomagenesis in Igλ-Myc mice. *Oncotarget*. 2015;6(24):20302-20311.

46. Saintamand A, Saad F, Denizot Y. 3'RR targeting in lymphomagenesis: a promising strategy? *Cell Cycle*. 2015;14(6):789-790.

47. Lindström MS, Wiman KG. Role of genetic and epigenetic changes in Burkitt lymphoma. *Semin Cancer Biol*. 2002;12(5):381-387.

48. Berg T, Thoene S, Yap D, et al. A transgenic mouse model demonstrating the oncogenic role of mutations in the polycomb-group gene EZH2 in lymphomagenesis. *Blood*. 2014;123(25):3914-3924.

49. Lue JK, Prabhu SA, Liu Y, et al. Precision targeting with EZH2 and HDAC inhibitors in epigenetically dysregulated lymphomas. *Clin Cancer Res*. 2019;25(17):5271-5283.

50. Lu ZP, Ju ZL, Shi GY, Zhang JW, Sun J. Histone deacetylase inhibitor Trichostatin A reduces anti-DNA autoantibody production and represses IgH gene transcription. *Biochem Biophys Res Commun*. 2005;330(1):204-209.

51. D'Addabbo P, Scascitelli M, Giambra V, Rocchi M, Frezza D. Position and sequence conservation in Amniota of polymorphic enhancer HS1.2 within the palindrome of IgH 3'Regulatory Region. *BMC Evol Biol*. 2011;11(1):71.